



Study the Structure of Phase Space in the Frame Work of Planar Circular Restricted Three-Body Problem

Kumar P* and Susmitha C

Department of Space Engineering, Ajeenkya D Y Patil University, India

*Corresponding author: Prashant Kumar, Department of Space Engineering, Ajeenkya D Y Patil University, Pune, India, 412105, Email: prashant1.rnsm@gmail.com

Review Article

Volume 2 Issue 2

Received Date: July 01, 2024

Published Date: July 17, 2024

DOI: 10.23880/oaja-16000120

Abstract

The numerical technique of Poincaré surface of sections is used to create the surface of sections and to investigate the stability of the phase plane in various systems. This includes investigating the dependence of mass ratio and amplitude of stability areas in the Sun-Jupiter, Sun-Mercury, Sun-Io, and Sun-Uranus systems on the Jacobi constant. The amplitude of the stability areas diminishes with decreasing mass ratio. The phase plane structure differs for smaller mass ratios than it does for larger mass ratios.

Keywords: Restricted Three-Body Problem; Poincaré Surface of Section; Phase Plane

Abbreviations

PSS: Poincaré Surface Section; KAM: Kolmogorov–Arnold–Moser.

Introduction

Poincaré surface of section (PSS) or simply surface of section is one of the fundamental and most visually exciting methods of evaluating the qualitative nature of a nonlinear dynamical system. The PSS method is a simple, yet effective technique that can display the qualitative nature of a dynamical system in a single diagram. This technique presents three essential features: The dimension reduction, global dynamics, and conceptual clarity. The use of PSS removes at least one variable in the dynamical system, resulting in the investigations and analysis of a lower-dimensional system.

Poincaré surface section (PSS) technique given by Poincaré H [1] is a widely used technique for analyzing periodic and quasi-periodic orbits in a qualitative way. Murray CD, et al. [2] has given a detailed analysis of periodic orbits using PSS. Chaotic behaviour of bodies can also

be studied using PSS, Liapunov characteristic numbers, Fourier transform techniques and numerical irreversibility technique. The set of stable periodic and quasi-periodic trajectories define regions of regular motion or stability islands that spread in a chaotic sea made up of trajectories with high sensitivity with respect to the initial condition.

As per Kolmogorov–Arnold–Moser (KAM) theory, each point of PSS represents a periodic orbit in the rotating frame, and the closed curves or islands around the point correspond to the quasi-periodic orbits.

Boucher K [3] demonstrates some of the aspects of chaos displaced by three-body problem, a circular Poincaré map and divergent solutions as well as explores how increasing Jupiter's mass affects the Earth's motion. Kolmen E, et al. [4] has employed multiple PSS method to find quasi-periodic orbits around the libration points L_1 and L_2 in the Sun–Earth system.

Beevi SA, et al. [5] has also studied PSS for Saturn–Titan system for periodic orbits, quasi-periodic orbits and chaotic orbits. Nishanth P, et al. [6] studied the interior resonance

periodic orbits around the Sun in the Sun-Jupiter PRTBP using the method of PSS. Kumar P, et al. [7] have used PSS technique to find the effect of solar radiation pressure of Sun on resonant periodic orbits in the frame work of planar circular restricted three body problem. Pathak N, et al. [8] explored the first-order exterior resonant orbits and the first, third, and fifth-order interior resonant periodic orbits within the setting of the perturbed photo-gravitational model. Kumar P, et al. [9] investigated the periodic orbits of smaller and larger primaries in the Sun-Jupiter and Sun-Earth systems, and discovered that the radiation force from the larger primary has a significant impact on eccentricity, orbit shape, size, and position in phase space.

The Equations of Motion

Consider the more massive primary of mass is m_1 and m_2 is the mass of the smaller primary. These two masses have

circular orbits about their common center of mass in a plane under the influence of their mutual gravitational attraction. A third body (attracted by the previous two but not influencing their motion) moves in the plane of primaries. To obtain the equations of motion for the third body, we choose XY as the sidereal frame and xy as the synodic frame. Let the coordinates of m_1 , m_2 and m in the sidereal frame be (X_1, Y_1) , (X_2, Y_2) and (X, Y) , respectively, and that in the synodic frame be (x_1, y_1) , (x_2, y_2) and (x, y) , respectively as shown in Figure 1. To non-dimensionalise the problem, take unit of mass the total of the masses of M_1 and M_2 , unit of length the distance between the primaries. These units force a gravitational constant $G = 1$. The only parameter in the system is the mass parameter μ .

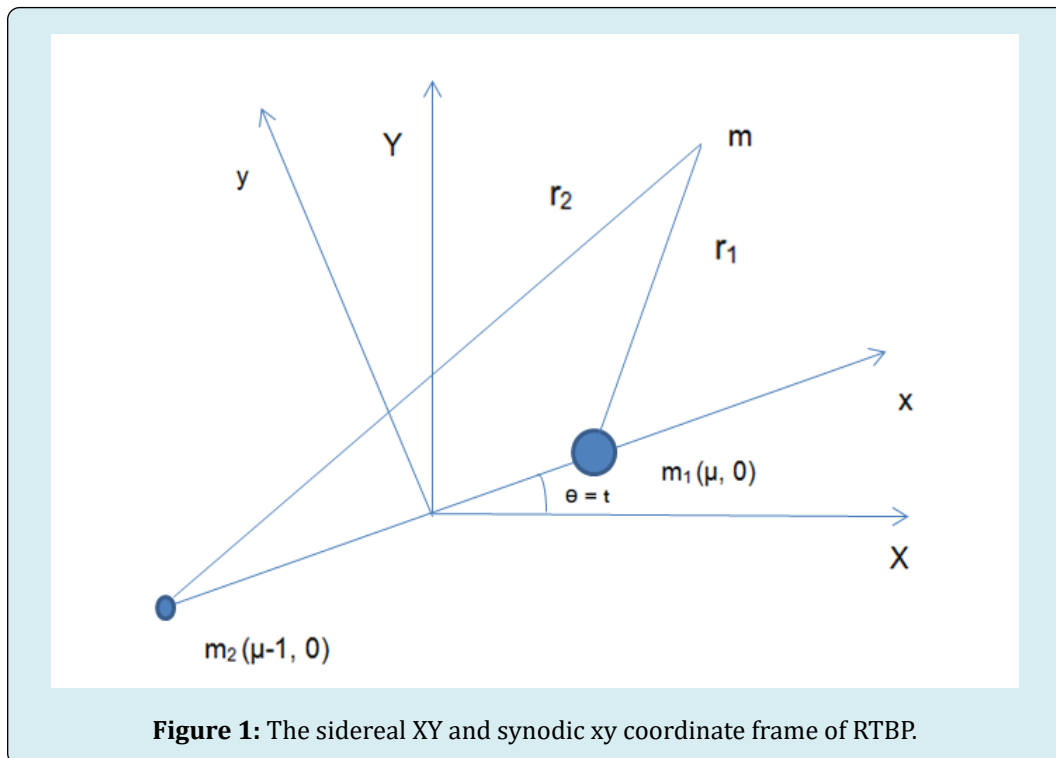


Figure 1: The sidereal XY and synodic xy coordinate frame of RTBP.

The transformation from synodic system (x, y) to sidereal system (X, Y) is given by

$$\begin{aligned} X &= x \cos t - y \sin t \\ Y &= x \sin t + y \cos t \end{aligned} \quad (7)$$

In the Sidereal Frame:

$$\text{Kinetic Energy } (T) = \frac{1}{2} [X^2 + Y^2] \quad (8)$$

$$\text{Potential Energy } (V) = - \left[\frac{1-\mu}{r_1} \right] - \frac{\mu}{r_2} \quad (9)$$

where r_1 and r_2 are the magnitudes of the position of the third body from the more massive primary and smaller primary, respectively.

The Lagrangian of the system is given as

- Lagrangian $(L) = \text{kinetic energy} - \text{potential energy}$

- Lagrangian (L) = $T-V$

$$= \frac{1}{2}[X^2 + Y^2] - \left[\frac{1-\mu}{r_1} \right] - \frac{\mu}{r_2} \quad (10)$$

Using equation (1), we get

$$\dot{X} = \dot{x} \cos t - x \sin t - \dot{y} \sin t - y \cos t \quad (11)$$

$$\dot{Y} = \dot{x} \sin t + x \cos t + \dot{y} \cos t - y \sin t$$

$$\dot{X}^2 + \dot{Y}^2 = (\dot{x} - y)^2 (\dot{y} + x)^2 \quad (12)$$

Equation (4) now take the form

$$\text{Lagrangian}(L) = \frac{1}{2}[(\dot{x} - y)^2 (\dot{y} + x)^2] + \left[\frac{1-\mu}{r_1} \right] - \frac{\mu}{r_2} \quad (13)$$

where

$$r_1^2 = (x - \mu)^2 + y^2 \quad (14)$$

$$r_2^2 = (x + 1 - \mu)^2 + y^2 \quad (15)$$

Differentiating r_1 and r_2 with respect to x and y , we get

$$\frac{\partial r_1}{\partial x} = \frac{x - \mu}{r_1} \quad (16)$$

$$\frac{\partial r_1}{\partial y} = \frac{y}{r_1}$$

$$\frac{\partial r_2}{\partial x} = \frac{x + 1 - \mu}{r_2} \quad (17)$$

$$\frac{\partial r_2}{\partial y} = \frac{y}{r_2}$$

Lagrange Equations:

$$\frac{d}{dt} \left(\frac{\partial L}{\partial \dot{x}} \right) - \frac{\partial L}{\partial x} = 0 \quad (18)$$

$$\frac{d}{dt} \left(\frac{\partial L}{\partial \dot{y}} \right) - \frac{\partial L}{\partial y} = 0 \quad (19)$$

where

$$\frac{\partial L}{\partial \dot{x}} = \dot{x} - y$$

$$\frac{\partial L}{\partial \dot{y}} = \dot{y} + x$$

$$\frac{\partial L}{\partial x} = \dot{y} + x - \frac{(1-\mu)(x-\mu)}{r_1^3} - \mu \frac{(x+1-\mu)}{r_2^3}$$

$$\frac{\partial L}{\partial x} = -\dot{x} + y - \frac{(1-\mu)y}{r_1^3} - \mu \frac{y}{r_2^3}$$

Lagrange equation corresponding to equation (18) is

$$\frac{d}{dt} [\dot{x} - y] - \left[\dot{y} + x - \frac{(1-\mu)(x-\mu)}{r_1^3} - \mu \frac{(x+1-\mu)}{r_2^3} \right] = 0$$

$$\dot{x} - 2\dot{y} = \left[x - \frac{(1-\mu)(x-\mu)}{r_1^3} - \mu \frac{(x+1-\mu)}{r_2^3} \right] \quad (20)$$

Let

$$\Omega = \frac{1}{2}(x^2 + y^2) + \left[\frac{1-\mu}{r_1} \right] + \frac{\mu}{r_2} \quad (21)$$

Equation (14) can be written as

$$\dot{x} - 2\dot{y} = \frac{\partial \Omega}{\partial n} \quad (22)$$

Lagrange equation corresponding to equation (19) is

$$\frac{d}{dt} [\dot{y} + x] + \left[-\dot{x} + y - \frac{(1-\mu)y}{r_1^3} - \mu \frac{y}{r_2^3} \right] = 0$$

$$\dot{y} + 2\dot{x} = \left[y - \frac{(1-\mu)y}{r_1^3} - \mu \frac{y}{r_2^3} \right]$$

$$\dot{y} + 2\dot{x} = \frac{\partial \Omega}{\partial y} \quad (23)$$

Jacobi Integral

Multiplying equation (16) by \dot{x} and equation (17) by \dot{y} , we get

$$\dot{x}\ddot{x} - 2\dot{y}\dot{x} = \dot{x} \frac{\partial \Omega}{\partial x} \quad (24)$$

$$y\ddot{y} - 2x\dot{y} = y \frac{\partial \Omega}{\partial y} \quad (25)$$

Adding equations (18) and (19), we get

$$\ddot{x} + \dot{y}\dot{y} = \frac{\partial x}{\partial t} \frac{\partial \Omega}{\partial x} + \frac{\partial y}{\partial t} \frac{\partial \Omega}{\partial y} \quad (26)$$

Integrating equation (20), we get

$$\frac{1}{2}\dot{x}^2 + \frac{1}{2}\dot{y}^2 = \Omega + C_1$$

$$\dot{x}^2 + \dot{y}^2 = 2\Omega + C \quad (27)$$

This is Jacobian integral. It will represent all possible motion for different values of Jacobi constant C.

Poincare Surface of Sections for Different Systems

The PSS method is a simple, yet effective technique that can display the qualitative nature of a dynamical system in a single diagram. A surface of section is found by viewing the trajectory in a stroboscopic manner. A great number of trajectories are to be computed for this technique [2]. In

this technique, the equations of motion (Eqn 22) and (Eqn 23) in chapter 1 were integrated using fourth-order Runge-Kutta-Gill method with integration step size Δt of 0.0005. The initial conditions were selected along the x-axis and the magnitude of the velocity vector was determined from its functional dependence on the Jacobi constant. The surface of section technique is good at determining the regular or chaotic nature of the trajectory. If there are smooth, well defined islands, then the trajectory is likely to be regular and the islands correspond to oscillation around a periodic orbit. The largest of the quasi-periodic orbits corresponds to the maximum amplitude of oscillation around the periodic one. The regular regions of a PSS are defined by a periodic orbit involved by quasi-periodic orbits and are interpreted as regions of stability in the sense that outside them the motion is certainly unstable and inside them the motion is in general regular. The maximum amplitude of oscillation is used as a parameter to measure the degree of stability of a periodic orbit with respect to the region around it in the phase space. Any fuzzy distribution of points in the surface of section implies that the trajectory is chaotic and within the mostly-chaotic regions, there are small regions of regular behavior, such as the region of interest indicated by the red circle as shown in Figure 2.1. Additionally, note that certain areas of the map display appear completely blank. No map returns exist in these areas because physical trajectories are not possible in these regions of the phase space.

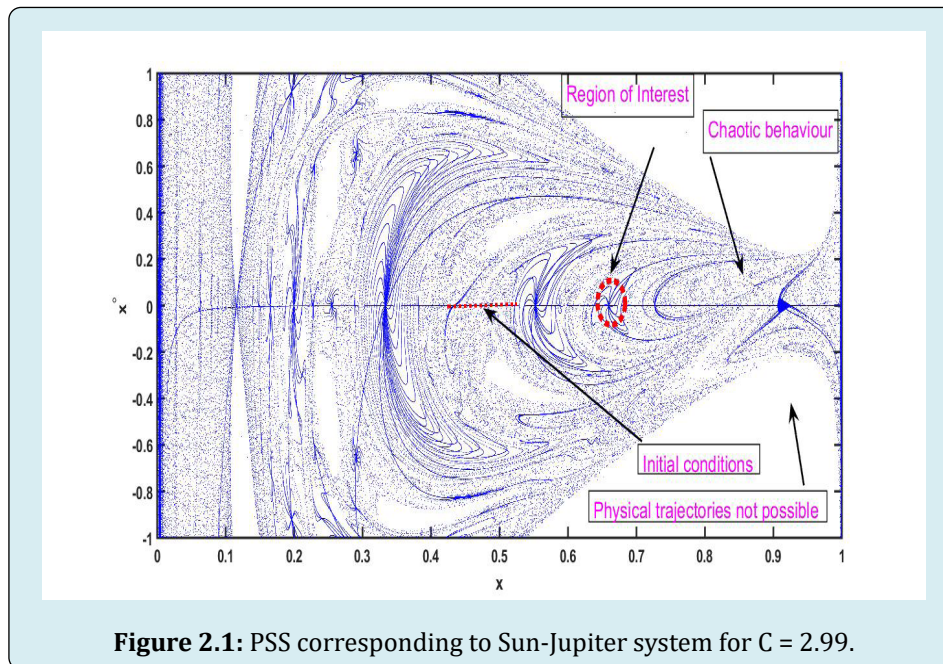


Figure 2.1: PSS corresponding to Sun-Jupiter system for $C = 2.99$.

To study the dependence of Jacobi constant and mass ratio for different systems on the stability regions, PSS at $C = 2.9$ and 3.0 are considered. Figures 2.2-2.9 shows the nature

of phase plane corresponding to the decreasing order of mass ratio from the Sun- Jupiter to the Sun- Mercury system. The PSS of Sun-Jupiter system with mass ratio 0.0009537284,

being the highest among the systems is generated for Jacobi constant $C = 2.9$ shown in Figure 2.2. In case of the fuzzy distribution of points, the region $x = 0.55$ to 0.65 is less for $C = 2.9$ and is more for $C = 3.0$. The stability region from $x = 0.6$ and 0.75 corresponding to the Jacobi constant $C = 2.9$ contain a number of invariant curves and with increase in the value of C from 2.9 to 3.0 , this stability region disappeared. The stability region at $x = 0.27$ for $C = 2.9$ correspond to the periodic orbit around the Sun and as C increases from 2.9 to 3.0 , this stability region moves towards the Jupiter.

The phase planes corresponding to the Sun-Uranus system given in Figures 2.2 & 2.3 show the number of invariant curves is less in each stability region. In case of the fuzzy distribution of points, it is more in the region from $x = 0.0$ to $x = 0.20$ for $C = 2.9$. The phase plots show that the stability region moves towards the right as C increases from 2.9 to 3.0 . Chains of several resonant islands are identified after $x = 0.75$ for $C = 2.9$ and as C increases to 3.0 , the size of

this resonant islands decreased.

The phase planes corresponding to the Jupiter-Io system are given in Figures 2.6 & 2.7. The phase plots show a number of islands with different size and shape and having comparatively small amplitudes with respect to the Sun-Jupiter system for Jacobi constant $C = 2.9$. In case of the fuzzy distribution of points, it is less in the region from $x = 0.3$ to $x = 0.70$ for $C = 2.9$ and is more for $C = 3.0$. Empty region is seen from $x = 0.7$ onwards, when C is increased from 2.9 to 3.0 .

Figure 2.8 gives the phase plane corresponding to the Sun-Mercury system for $C = 2.9$. Fuzzy distribution of points is more in the region from $x = 0.0$ to $x = 0.6$ and number of islands are less in the phase plane. As C increases to 3.0 , fuzzy distribution of points increased after $x = 0.7$. The stability regions after $x = 0.25$ move towards the Jupiter as C increases from 2.9 to 3.0 .

PSS for the Sun-Jupiter System

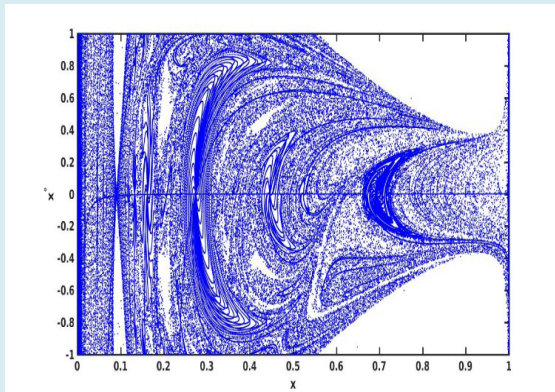


Figure 2.2: PSS for $C = 2.9$.

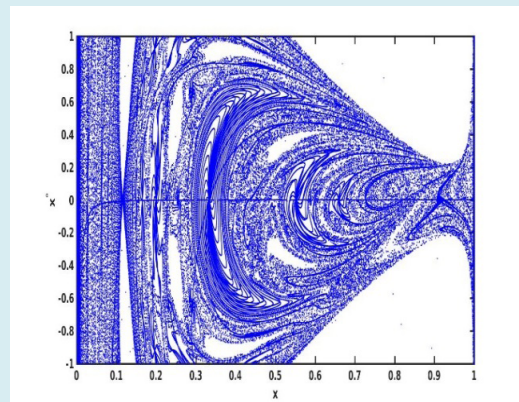


Figure 2.3: PSS for $C = 3.0$.

PSS for the Sun-Uranus System

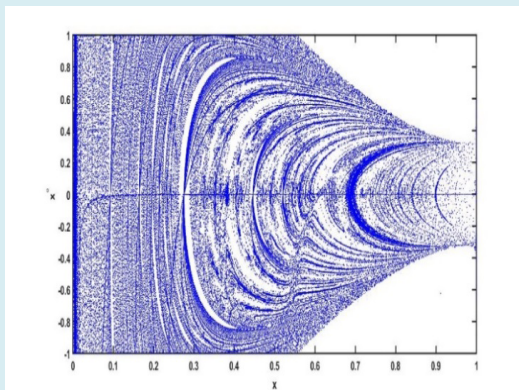


Figure 2.4: PSS for $C = 2.9$.

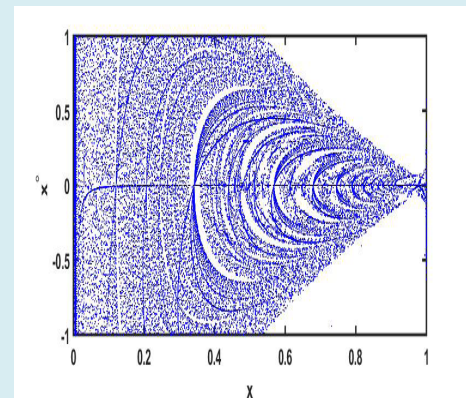


Figure 2.5: PSS for $C = 3.0$.

PSS for the Jupiter-I₀ System

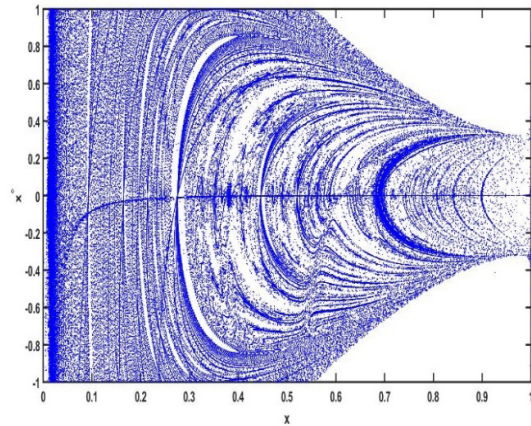


Figure 2.6: PSS for $C = 2.9$.

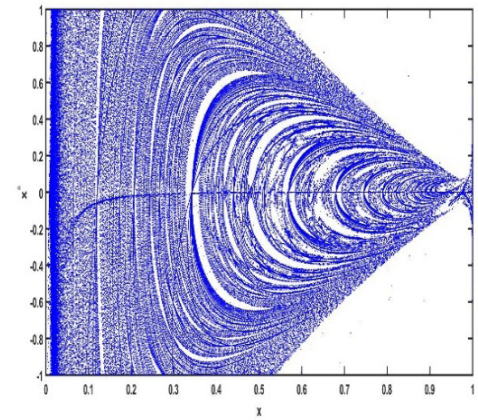


Figure 2.7: PSS for $C = 3.0$.

PSS for the Sun-Mercury System

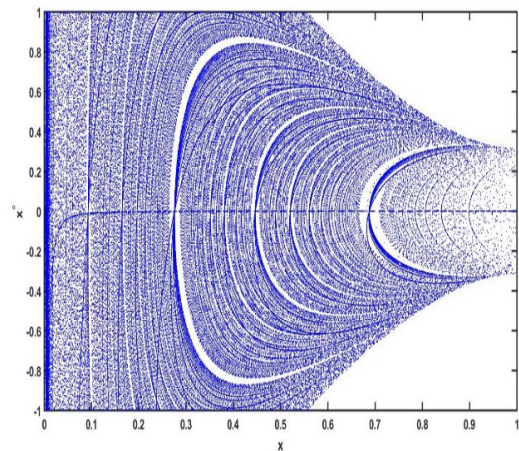


Figure 2.8: PSS for $C = 2.9$.

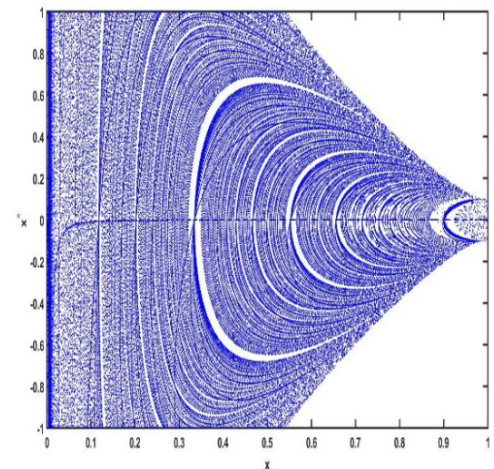


Figure 2.9: PSS for $C = 3.0$.

Conclusions

The numerical technique of Poincaré surface of sections is used to generate PSS and to study the location and stability of phase plane in various systems. The phase plane corresponding to the Jacobi constant at $C = 2.9$ and 3.0 in descending order of mass ratio are presented. As mass ratio decreases, the amplitude of the stability regions decreases. For smaller mass ratios, the structure of the phase plane is in a different manner than that of the higher mass ratios. The stability regions move towards the smaller as C increases from 2.9 to 3.0 .

References

1. Poincare H (1892) The New Methods of Celestial Mechanics. In: Goroff D (Ed.), History of Modern Physics and Astronomy, France 1: 82.
2. Murray CD, Dermot SF (1999) Solar System Dynamics. Cambridge University Press.
3. Boucher K (2004) The restricted three-body problem. Phys, Hamiltonian Dynamics 349: 1-27.
4. Kolmen E, Kasdin NJ, Gurfil P (2007) Quasi-periodic

orbits of the restricted three-body problem made easy. New trends in astrodynamics and applications. American Inst of Physics, USA 886: 68-77.

5. Beevi SA, Sharma RK (2011) Analysis of periodic orbits in the Saturn–Titan system using the method of Poincare section surfaces. *Astrophysics and Space Science* 333: 37-48.
6. Nishanth P, Sharma RK (2017) Interior Resonance Periodic Orbits in Photogravitational Restricted Three-body Problem. *Advances in Astrophysics* 2(1): 263-272.
7. Kumar P, Sharma RK (2019) On merging of resonant periodic orbits 4:3; 3:2 and 2:1 in Sun-Jupiter photo gravitational restricted three-body problem. *International Journal of Advanced Astronomy* 7(1): 17-24.
8. Kumar P, Gupta ESD, Mourya MKJ, Pranav SV (2023) Evolution of Periodic Orbits in the Sun-Jupiter and Sun-Earth Systems. *Indian journal of science and technology* 16(10): 717-726.
9. Pathak N, Thomas VO, Abouelmagd I (2019) The perturbed photogravitational restricted three body problem: Analysis of resonant periodic orbits. *Discrete and continuous dynamical systems series* 12(4-5): 849-875.